Reactivity of (*NNN*)-pincer nickel(II) aryl complex towards oxidative carbon-heteroatom bond formation

Felipe C. Sousa e Silva, Brandon J. Bloomer, Sarah E. Wengryniuk

PII: S0040-4020(18)30408-3

DOI: 10.1016/j.tet.2018.04.029

Reference: TET 29444

To appear in: *Tetrahedron*

Received Date: 16 January 2018

Revised Date: 10 April 2018

Accepted Date: 11 April 2018

Please cite this article as: Sousa e Silva FC, Bloomer BJ, Wengryniuk SE, Reactivity of (*NNN*)-pincer nickel(II) aryl complex towards oxidative carbon-heteroatom bond formation, *Tetrahedron* (2018), doi: 10.1016/j.tet.2018.04.029.

Graphical Abstract

To create your abstract, type over the instructions in the template box below.

Fonts or abstract dimensions should not be changed or altered.

Reactivity of (*NNN*)-pincer Ni(II) aryl complex towards oxidative carbon-heteroatom bond formation

Leave this area blank for abstract info.

Felipe C. Sousa e Silva, Brandon J. Bloomer, Sarah E. Wengryniuk*
Temple University, Department of Chemistry, 1901 North 13th Street, Philadelphia, PA 19122, USA

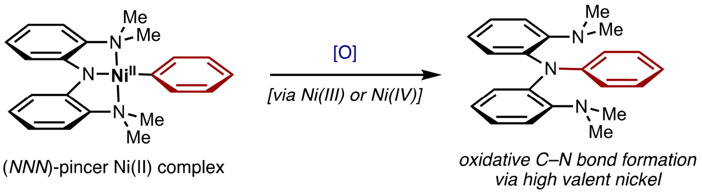

Tetrahedron
journal homepage: www.elsevier.com

Reactivity of (*NNN*)-pincer nickel(II) aryl complex towards oxidative carbon-heteroatom bond formation

Felipe C. Sousa e Silva[a], Brandon J. Bloomer[b], and Sarah E. Wengryniuk[a]*

[a]*Temple University, Department of Chemistry, 1901 North 13th Street, Philadelphia, PA, 19122, USA*
[b]*Department of Chemistry, University of California, Berkeley, Berkeley, California 94720, USA*

ARTICLE INFO

Article history:
Received
Received in revised form
Accepted
Available online

Keywords:
nickel
pincer
high-valent
carbon-heteroatom
oxidative
carbon-nitrogen

ABSTRACT

The reactivity of an (*NNN*)-Ni(II) aryl complex towards C–X bond formation upon exposure to a panel of one- and two-electron oxidants is reported. High selectivity for C(sp^2)–N bond formation is observed in all cases, except under conditions when C–C bond formation is accessible. Preliminary mechanistic investigations indicate access to either a Ni(III) or Ni(IV) intermediate dependent on oxidant used and that C–N bond formation is more efficient via Ni(IV) pathway due to geometry of reactive species.

---

* Corresponding author. Tel.: +1-215-204-0360; e-mail: sarahw@temple.edu

1. Introduction

Over the last decade, the field of high-valent metal catalysis has emerged as a new and powerful tool in organic synthesis. In particular, high oxidation state metal centers can facilitate challenging C–X bond forming reductive eliminations, including carbon-halogen, carbon-oxygen, and carbon-nitrogen bond formation.[1,2] While palladium catalysis has played a central role in this field over the last 20 years, there has been a growing interest in C–X bond forming reactions from high-valent nickel intermediates.[3-8] The development of analogous nickel-catalyzed methods would be particularly attractive as nickel is more economical and sustainable, however significant challenges still remain.[9] Firstly, nickel can undergo facile one- or two-electron redox events allowing access to both Ni(II)/Ni(III) or Ni(II)/Ni(IV) manifolds, hindering reaction development due to limited mechanistic understanding.[5,6] Second, the relatively low stability of high-valent nickel centers makes the design of ligand scaffolds capable of stabilizing these intermediates and facilitating efficient catalyst turnover challenging, particularly at the Ni(IV) oxidation state.[10] Thus, there are continued efforts towards the design, synthesis and characterization of high-valent nickel complexes to probe their reactivity towards C–X bond formation, providing key insights for the development of catalytic manifolds. [11-13]

In this area, seminal work from the Hillhouse group has shown that cyclic Ni(II) complexes possessing alkyl and amido ligands undergo facile $C(sp^3)$–N reductive elimination upon exposure to one-electron oxidants including O_2, I_2, or $[(AcCp)Fe]^+$, via a Ni(III) intermediate.[14-16] Recent mechanistic investigations from the Sanford group have reported the synthesis and isolation of several stable Ni(II) precursors and the study of their reactivity upon exposure to a range of one- and two-electron oxidants under stoichiometric conditions.[3,5,10,17,18] In 2009 they reported that (phpy)(picoline)Ni(II)Br complex **1** (phpy=2-phenylpyridine) underwent efficient C–Br bond formation upon treatment with either Br_2 or $CuBr_2$, via a proposed Ni(III) intermediate (Scheme 1A).[3] Subsequently, bis(phpy)Ni(II) species **7**, was found to undergo preferential C–C bond formation to give **4** along with trace C–Br (**3**) and C–N (**6**) products upon oxidation with N-bromosuccinimide (Scheme 1B). Although no high-valent nickel species were characterized, an analogous Pd(IV) species gave a similar product distribution, suggesting the possible intermediacy of a Ni(IV) species.[4,19] In a recent high profile report, Sanford employed $[(bpy)Ni^{II}(CH_2CMe_2\text{-}o\text{-}C_6H_4)]$ complex **7** and found that upon oxidation by several $2e^-$ oxidants (**10-13**), **7** underwent selective C–C bond formation with no evidence of competitive C–X reductive elimination products.[5] Significantly, use of a more stabilizing tridentate tris(2-pyridyl)methane (tppp) ligand system enabled the isolation and full characterization of key Ni(IV) intermediates for the first time, suggesting the feasibility of this redox manifold for C–X bond formation. Subsequent studies from the Sanford lab have utilized **7**, the (tppp)-ligand system and a closely related trispyrazolylborate scaffold to examine a range of C–X and C–C bond forming processes, providing key mechanistic insights towards the feasibility of catalytic manifolds.[5,10,17,18] Ritter has reported an oxidative radiofluorination method employing stoichiometric Ni(II)–aryl complexes, which upon exposure to a hypervalent iodine oxidant and nucleophilic fluoride, underwent smooth $C(sp^2)$–F reductive elimination, presumably via a Ni(IV) intermediate.[8] The Muniz group reported the first example of *catalytic* $C(sp^3)$–N bond formation from a proposed Ni(III) intermediate in an approach to oxidative olefin diamination (Scheme 1D).[20]

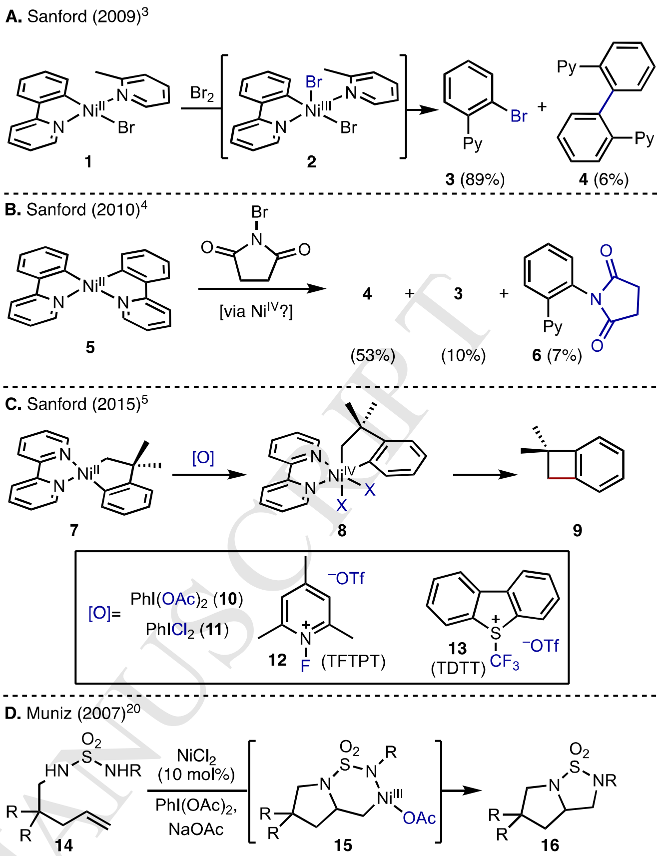

Scheme 1. **A.** Oxidative C–Br bond formation via proposed Ni(III) intermediate **B.** Preferential oxidative C–C coupling along with trace C–Br and C–N products from bis(phpy)Ni(II) complex. **C.** Selective C–C coupling from Ni(IV) intermediate **D.** First example of catalytic C–N bond formation via proposed Ni(III) intermediate.

In an effort to explore new ligand scaffolds that could enable catalytic, oxidative C–X bond formation via either Ni(III) or Ni(IV), we were drawn to the amido bis(amine) pincer Ni-complexes recently developed by Hu (**17**, **18**, Scheme 2). By replacing the phosphorous atoms of established PNP-pincer ligands with nitrogens, Hu aimed to increase the relative “hardness” in order to better stabilize high-oxidation state metal complexes. To date Hu has successfully utilized *(NNN)*-NiCl complex **17** for a wide variety of nickel-catalyzed $C(sp^3)$ Kumada couplings.[21-31] A detailed mechanistic investigation led to the conclusion that the Kumada coupling proceeds via a Ni(III) intermediate (**19**), accessed via radical oxidation of the Ni(II) center by an aryl iodide after transmetallation (Scheme 2B).[29] However, despite its utility in catalytic C–C bond formation, there have been no reports examining the viability of the (*NNN*)-pincer scaffold to enable analogous C–X bond forming processes via high-valent nickel intermediates. Herein, we report a study of the reactivity of *(NNN)*-NiPh complex **18** upon treatment with a range of both one and two-electron oxidants (Scheme 2C). Our studies have found that **18** will undergo preferential $C(sp^2)$–N bond formation over competitive carbon-oxygen or carbon-halogen pathways, however carbon-carbon bond formation will predominate upon exposure to an appropriate oxidant. Preliminary mechanistic studies indicate the role of either Ni(II)/Ni(III) or Ni(II)/Ni(IV) redox manifolds depending on the oxidant used and our results indicate that C–N bond formation is more efficient through the proposed Ni(IV) pathway. The findings indicate the viability C–N bond reductive elimination from high-valent nickel complexes, most notably Ni(IV), and reveal the significant role that oxidant selection plays in reaction development, providing valuable insights for further catalytic development.

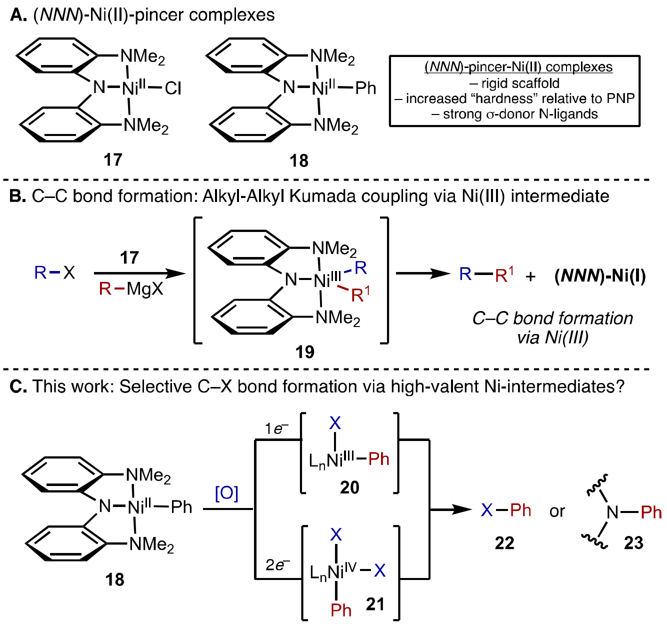

Scheme 2. A. (*NNN*)-pincer Ni(II) complexes developed by Hu. **B.** Use of **17** for alkyl-alkyl Kumada coupling via Ni(III) intermediate. **C.** This work: examining the reactivity of **18** towards oxidative C–X bond formation.

2. Results and Discussion

Our studies focused on the reactivity of (*NNN*)-NiPh complex **18**, which was readily prepared according to the procedure reported by Hu.[32] We hypothesized that, depending on the nature of the oxidant, this could give rise to either a Ni(III) (**20**) or Ni(IV) (**21**) intermediate, stabilized by the strong σ-donor nitrogen-ligands (Scheme 2C). These intermediates could then either undergo reductive C–X bond formation, where X would arise from the oxidant, to give **22**, or reductive C–N bond formation onto the ligand scaffold (**23**). Significantly, complex **23** does not have the ability to undergo a competitive C–C bond reductive elimination, a pathway found to outcompete C–X bond formation in previous studies of high-valent nickel intermediates.[3-5,8,10,17,18]

We began by exposing **18** to a panel of well-established $2e^-$ electron oxidants, including λ^3-iodanes (tolyl)I(OAc)$_2$, (tolyl)ICl$_2$, and [PhI(Py)$_2$]2OTf, as well as NCS and TDTT (Table 1, entires 1-6).[3-5,8,33,34] In each case we observed exclusive formation of **23** in near quantitative yield, the product of clean C(sp^2)–N bond formation.[35] Surprisingly, no products arising from competitive C–X reductive elimination onto the arene were observed (i.e. **22**) either by GCMS or ^{1}H-NMR of the crude reaction mixtures.[36] While there are reports of C(sp^3)–N bond formation via Ni(III),[14-16,20] and C(sp^2)–N bond formation has been reported via Pd(II)/Pd(IV),[37] to the best of our knowledge there exists only one report of C(sp^2)–N reductive elimination from a high-valent nickel species,[38] and our finding is in contrast to Sanford's observation in which only trace C–N bond formation was observed upon oxidation of **5** with NBS (see Scheme 1B).[4] We then examined both outer-sphere ((FeCp$_2$)PF$_6$) and inner-sphere (CuCl$_2$) $1e^-$ oxidants (entries 7, 8), both of which proved less efficient at promoting C–N bond formation than the $2e^-$ reagents. (FeCp$_2$)PF$_6$ gave lower conversion to **23**, with a 1:0.42 ratio of **23** with starting complex **18** (entry 7). In contrast, CuCl$_2$ gave full consumption of starting complex **18**, however produced a 1.0:0.91 ratio of **23** to (*NNN*)-NiCl complex **17**. We were intrigued by this drop in reaction efficiency upon use of one-electron oxidants as Ni(II)/Ni(III) pathways had been reported for C–N bond forming reductive eliminations previously.[2,12-14,18] These results indicate that in our system, a potential Ni(II)/Ni(IV) pathway was more efficient at promoting of C–N bond formation (see later for further discussion).

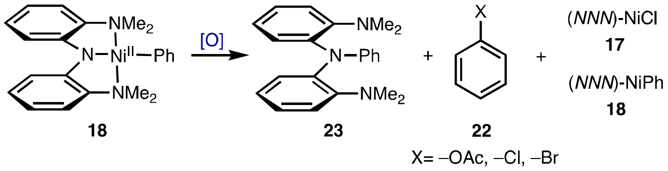

Table 1. Oxidation of **18** with both one- and two-electron oxidants

Entry	Conditions[a]	Product Distribution[b]	Yield **23** (%)[c]
1	(tolyl)I(OAc)$_2$	**23** only	94
2	(tolyl)ICl$_2$	**23** only	99
3	[PhI(Py)$_2$]2OTf	**23** only	99
4	NCS	**23** only	98
5	NBS	**23** only	96
6	TDTT	**23** only	98
7	Fe(Cp$_2$)PF$_6$	1:0.42 (**23**:**18**)	--[c]
8	CuCl$_2$	1:0.91 (**23**:**17**)	52

[a] Reactions were carried out in dry THF with exception of the entry 8: THF/ACN 1:1 v/v. [b] Initial product distributions determined via ^{1}H-NMR of crude reaction mixtures. [c] Isolated yield of **23** determined after column chromatography. [d] Isolated yield of **23** not obtained as remaining **18** degrades to **23** upon purification.

Having established the tendency of **18** to undergo highly selective C–N over competitive C–X pathways, we wished to examine C–N vs. C–C coupling (Scheme 3). C–C bond formation has been established as the major pathway in prior studies of high-valent nickel species[3–5,10,17,18] (*vide supra*) and Hu's studies have revealed a Ni(III) intermediate for his highly efficient Kumada coupling using **17**.[29] We would therefore predict C–C coupling to predominate over C–N coupling upon exposure to $2e^-$ oxidant such as an aryl halide, aryldiazonium, or diaryliodonium salt.[18] In fact, treatment of **18** with diaryliodonium salt **24** gave biaryl **25** as the major product in 30% yield, along with 9% yield of C–N product **23**, with remaining mass balance accounted for by free (*NNN*)-ligand.[39] While the C–C coupling proceeded in only moderate yield, this result supports the previous observations that in high-valent nickel intermediates where C–X vs. C–C coupling pathways are competitive, C–C coupling is preferred and thus this should be avoided for the design of future ligand scaffolds for C–X bond formation.

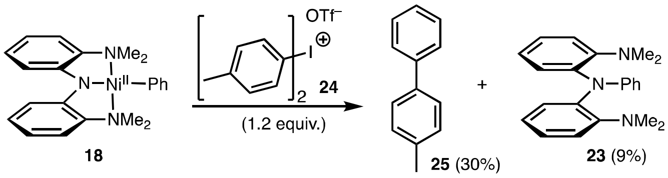

Scheme 3. Preferential C–C coupling, leading to biaryl formation upon oxidation with diaryliodonium salt **24**.

At this stage we wished to probe the mechanistic underpinnings for the drop in C–N bond efficiency between $2e^-$ oxidants (Table 1, entries 1-7) and $1e^-$ oxidant (CuCl$_2$, entry 8), with the hypothesis that this may result from a switch in reaction manifold from Ni(II)/Ni(IV) to Ni(II)/Ni(III). The differential pulse voltammogram of **18** revealed two oxidative peaks, at

+0.75V and +1.39V versus Ag/Ag$^+$, which we assign to the Ni(II)/(III) and Ni(III)/(IV) redox couple, respectively. Both oxidations display quasi-reversible behavior, however complex degradation appears much more significant upon oxidation to Ni(IV) (see Supporting Information for details and further discussion). We then attempted the use of various additives to probe potential one-electron pathways, unfortunately, addition of TEMPO or BHT resulted in no change in reaction outcome and no detectable formation of adducts in the case of any of the oxidants screened.[18] Furthermore, attempts to isolate or observe any high-valent nickel intermediates by NMR were unsuccessful due to instability and rapid rate of C–N bond formation from these species even at low temperature. We therefore attempted to gain insights into the reaction pathways by altering the equivalents of respective oxidants added (Scheme 4). In order to confirm the $CuCl_2$ result, we turned again to (tolyl)ICl_2, which is commonly viewed as a 2e^- oxidant, however use of 0.5 equiv. can result in each equivalent performing two 1e^- oxidations, as demonstrated by Nocera in the oxidation of a (dppe)Ni(II)Cl_2 complex to (dppe)Ni(III)Cl_3.[40] Treatment of **18** with 0.5 equiv. of (tolyl)ICl_2 resulted in complete consumption of starting material and analysis of the ^{1}H-NMR of the crude reaction revealed a 1.0:1.01 ratio of C–N product **23** to (*NNN*)-NiCl (**17**) (Scheme 4A).[41] This result is significantly different than the oxidation with 1 equiv. (Table 1, entry 2) and analogous to the results obtained with $CuCl_2$. Next, to probe the 2e^- oxidation, we treated **18** with 0.5 equiv. of [PhI(Py)$_2$]2OTf and in this case we observed a 1.03:1.0 ratio of C–N product (**23**) to unreacted starting complex **18** (Scheme 4B).[42] This result would indicate that each equivalent of [PhI(Py)$_2$]2OTf is performing a net 2e^- oxidation of a single Ni(II) center to Ni(IV) as 1 equiv. gave near quantitative yield of **23**. While the above results are not definitive evidence, they are supportive of divergent reaction pathways dependent on the oxidation state of the reactive nickel species and provide preliminary evidence for a Ni(II)/Ni(IV) redox couple being more efficient for the formation of C–N bond products.

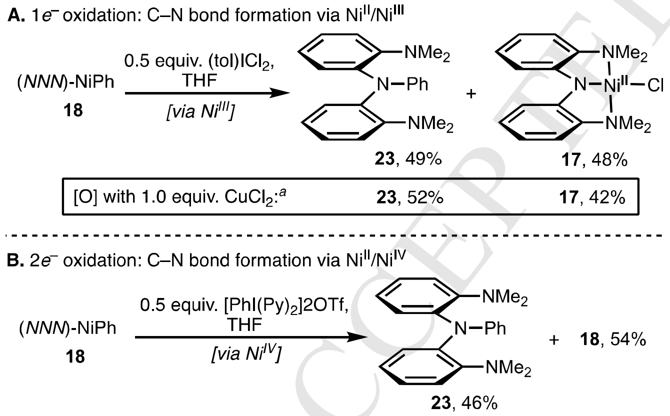

Scheme 4. Mechanistic probe into the efficiency of Ni(III) vs. Ni(IV) intermediates in C–N bond formation. [a]Ratio confirmed by isolated yields after chromatography. **17** isolated as free (*NNN*)-ligand. See SI for details.

We hypothesize that the divergence in C–N bond efficiency between the proposed Ni(IV) and Ni(III) pathways can be explained based on the geometries of the two nickel species upon oxidation (Scheme 5). Due to the relative instability of the high-valent nickel species, the initial geometry obtained upon oxidation could play a central role in the favored reaction pathway. Treatment with a 2e^- oxidant results in *cis*-addition of two X-groups to the nickel center to give **21**,[5] forcing the phenyl group into an axial position, *cis* to the nitrogen, and facilitating rapid C–N bond reductive elimination.[43] In contrast, 1e^- oxidation gives a Ni(III) species (**20**) which must undergo an isomerization to access a species (**26**) capable of C–N bond formation. However, prior to isomerization, **20** can undergo homolysis of the labile Ni–Ar bond, giving rise to Ni(II)–Cl species **17** and an aryl radical gives benzene after H-atom abstraction, presumably from THF solvent.[44] We believe these findings could provide valuable insights to address issues of reaction efficiency and selectivity in the continued development of nickel-mediated oxidative C–X bond formations.

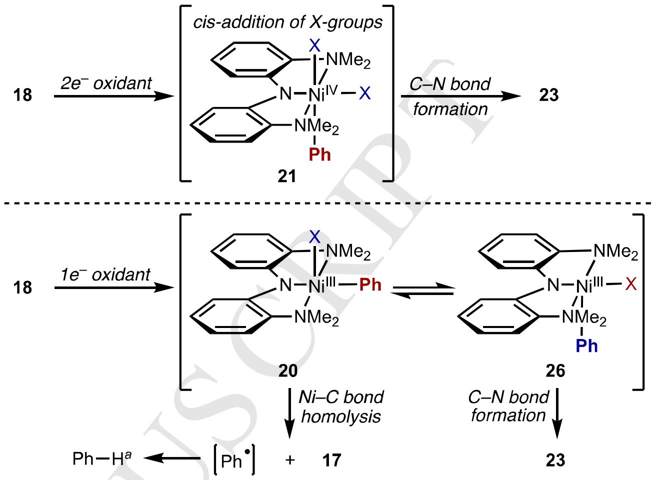

Scheme 5. Role of complex geometry on efficiency of C–N bond formation. [a]Detected via GC analysis of the crude reaction mixture under conditions shown in Scheme 4A. See Supporting Information for details.

3. Conclusion

In conclusion, we report the reactivity of an (*NNN*)-NiPh complex towards oxidative C–X bond formation. Our studies have shown that this complex undergoes highly selective C(sp^2)–N bond formation over competitive carbon-halogen or carbon-oxygen reductive elimination pathways, resulting in functionalization of the ligand scaffold. Alternatively, (*NNN*)-NiPh will undergo preferential C–C bond formation upon treatment with a diaryliodonium salt, in line with previous reports on the reactivity of high-valent nickel complexes. Preliminary mechanistic studies indicate that C–N bond formation is more facile via a Ni(II)/Ni(IV) pathway than Ni(II)/Ni(III), which we hypothesize is due to the differences in geometries of the resultant high-valent complexes. This transformation represents one of the first examples of C(sp^2)–N reductive elimination from a proposed Ni(IV) intermediate and we believe that these findings could aide in the continued pursuit of catalytic C–X bond forming manifolds via high-valent nickel intermediates.

4. Experimental section

4.1. General Information

^{1}H and ^{13}C NMR spectra were recorded at 500 MHz and 125 MHz on a Bruker Advance 500 or 400 MHz and 100 MHz on a Bruker Advance 400. ^{1}H NMR chemical shifts were reported in part per million (ppm) from the solvent resonance ($CDCl_3$ 7.26 ppm, C_6D_6 = 7.16 ppm). The data was reported as follows: chemical shift number, multiplicity (s = singlet, d = doublet, t = triplet, sept = septet, dd = doublet of doublets, td = triplet of doublets, m = multiplet). Proton decoupled attached proton test (APT) ^{13}C NMR shifts were reported in ppm from the solvent resonance ($CDCl_3$ 77.16 ppm). The reaction solvents used were anhydrous (HPLC-grade solvent passed through an activated-alumina column). All other reagents were used without further purification. $[(Py)_2IPh]2OTf$ and $[Tol_2I]OTf$ were synthesized according to the literature,[46,47] and used without further purification. Flash chromatography was carried out using Sorbent Technologies silica gel 60 6 (40 — 63 pm) in the solvent system listed in the individual experiments. The reactions were monitored using analytical thin-layer chromatography (TLC) on Merck silica gel (60 F2s4) plates. Accurate mass spectra were recorded on an Agilent 6520 Accurate-Mass Q-TOF LC/MS. All reactions were carried out inside glovebox unless specified.

*4.2. Synthesis of (NNN)-NiPh Complex (**18**)*

*4.2.1. Synthesis of Bis[dimethylamino)phenyl]amine ($H^{Me}NN_2$)(**SI-1**)*

Inside a glovebox, a 250 mL reaction vessel was charged with $Pd_2(dba)_3$ (1.36 g, 1.49 mmol), bis(diphenylphosphino)-ferrocene (DPPF) (1.65 g, 2.97 mmol), NaO*t*-Bu (9.84 g, 0.098 mol) and toluene (100 mL). 2-Bromo-N,N-dimethylaniline (14.6 g, 0.073 mol) and 2-amino-N,N-dimethylaniline[40] (9.95 g, 0.073 mol) were degassed and added to the reaction mixture. The brown solution was then stirred for 3 days at 100 °C. The solution was then cooled to room temperature and filtered through Celite. Removal of the solvent yielded a dark liquid that was taken in dichloromethane (20 mL) and filtered through a silica plug. Removal of the solvent gave **SI-1** as a brown solid (12.0 g, 0.048 mol, 66%) that was used without further purification. Spectral data was consistent with that reported in the literature.[48]

*4.2.2. Compound **17***

In a flame dried flask, under Ar, $H^{Me}NN_2$ (**SI-1**) (0.50 g, 2.0 mmol) was dissolved in THF (6 mL) and the solution cooled to –78 °C. *n*-BuLi (0.80 mL, 2.1 mmol, 2.5 M in hexanes) was added to the solution dropwise. The solution was allowed to warm naturally and stir for 1 h at room temperature. The resultant solution was then transferred to a THF (6 mL) suspension of $NiCl_2(dme)$ (0.44 g, 2.0 mmol) at –78 °C. The reaction was allowed to warm naturally and was left stirring overnight at room temperature[26]. The solvent was then removed and the dark brown oil was taken in benzene and filtered through celite. The brown oil was purified by recrystallization (layer diffusion of pentane in benzene at room temperature) to give *(NNN)*-NiCl (**17**) as a brown solid (0.52 g, 1.5 mmol, 74%). Spectral data was consistent with that reported in the literature.[32]

*4.2.3. Compound **18***

Inside a glovebox, PhMgBr (0.72 mL, 1 M solution in THF) was added dropwise to a THF (5 mL) solution of *(NNN)*-NiCl (**17**) (0.25 g, 0.72 mmol) at –78 °C. The resultant solution was allowed to warm naturally to room temperature and stirred overnight. The solvent was removed *in vacuo* and the dark residue was then dissolved in benzene (30 mL) and filtered through Celite. The solvent was removed *in vacuo* to afford **18** as a yellow solid, which was purified by recrystallization (layer diffusion of pentane in THF) to give **18** (0.17 g, 0.45, 62%). Spectral data was consistent with that reported in the literature.[32]

*4.3. General procedure for oxidation of (NNN)-NiPh **18**:*

Inside a glovebox, (*NNN*)-NiPh (15.0 mg, 0.04 mmol, 1 equiv.) and the appropriate oxidant (1.0-1.2 equiv.) were added to a 20 mL scintillation vial. THF(1.0 mL) was added to give a 0.04 M solution and the mixture was allowed to stir overnight at room temperature. The vial was brought outside the glovebox and the solvent was removed *in vacuo*. Initial product ratios of **23**:**22**:**17** were evaluated via analysis of the crude ^1H-NMR spectra (see Supporting Information for details). Isolated yields of **23** were obtained following purification by flash chromatography (5% EtOAc/Pentane).

*4.3.1. Compound **23***

Isolated as a pale yellow crystalline solid. ^1H NMR (500 MHz, $CDCl_3$): δ 7.11 – 7.07 (m, 2H), 7.05 – 7.01 (m, 4H), 6.97 – 6.94 (m, 2H), 6.88 – 6.82 (m, 3H), 6.81 – 6.77 (m, 2H), 2.45 (s, 12H). ^{13}C NMR (125 MHz, $CDCl_3$): δ 148.04, 138.86, 128.02, 127.35, 123.98, 121.65, 120.12, 119.38. HRMS (ESI) *m/z*: $C_{22}H_{25}N_3^+$ $[(M + H)^+]$ calcd: 332.2127, found: 332.2122. X-ray crystallographic data for **23** is provided in Supporting Information (**SI-12**).

*4.4. C–C bond formation: Oxidation with diaryliodonium salt **24**:*

Inside a glovebox, (*NNN*)-NiPh (15.0 mg, 0.04 mmol) was added to a 20 mL scintillation vial and dissolved in a 1:1 mixture of THF/CH_3CN (1 mL total volume, 0.04 M). $[Tol_2I]OTf$ was added in one portion and the solution was then stirred overnight at room temperature. The vial was brought outside the glovebox and the solvent was removed *in vacuo*. The reaction was purified by flash chromatography (5% EtOAc/Pentane) to yield **25** (2.0 mg, 0.012 mmol, 29%), **23** (1.6 mg, 0.004 mmol, 9.2%), and $H^{Me}NN_2$ (**27**) (5.4 mg, 0.024 mmol, 60%). Spectral data for **25** was consistent with that reported in the literature.[45]

4.5. Mechanistic Investigation

4.5.1. Oxidation with 0.5 equiv. of $(tolyl)ICl_2$

Inside a glovebox, (*NNN*)-NiPh (**18**) (10 mg, 0.025 mmol, 1 equiv.) and $(tolyl)ICl_2$ (3.6 mg, 0.0125 mmol, 0.5 equiv.) were added to a 20 mL scintillation vial. THF (1 mL, 0.025 M) was added and the mixture was allowed to stir overnight at room temperature. The solvent was removed *in vacuo* inside the glove box. Still inside the glovebox, the crude mixture was dissolved in C_6D_6, filtered and added to a NMR tube. Analysis of the ^1H-NMR spectra of the crude reaction mixture revealed **23**:**17** in a 1.0:0.91 ratio, along with trace impurities relating to $(tolyl)ICl_2$ (see Supporting Information for full details).

4.5.2. Oxidation with 0.5 equiv. of $[PhI(Py)_2]2OTf$

Inside a glovebox, (*NNN*)-NiPh (**18**) (10 mg, 0.025 mmol, 1 equiv.) and $[PhI(Py)_2]2OTf$ (8.3 mg, 0.0125 mmol, 0.5 equiv.) were added to a 20 mL scintillation vial. THF (1 mL, 0.025 M) was added and the mixture was allowed to stir overnight at room temperature. The solvent was removed *in vacuo* inside the glove box. Still inside the glovebox, the crude mixture was dissolved in C_6D_6, filtered and added to a NMR tube. Analysis of the ^1H-NMR spectra of the crude reaction mixture revealed only **23**:**17** in a 1.03:1.0 ratio, along with trace impurities relating to $[PhI(Py)_2]$ 2OTf (see Supporting Information for full details).

Acknowledgments

The authors would like to acknowledge the Donors of the American Chemical Society Petroleum Research Fund for partial support of this research (DNI-56603) as well the Temple University Department of Chemistry. B.J.B. was supported in part by the Temple University Undergraduate Research Program. Support for the NMR facility at Temple University by a CURE grant from the Pennsylvania Department of Health is gratefully acknowledged. We also thank Dr. Charles DeBrosse (Temple

University) for NMR spectroscopic assistance, the Zdilla group (Temple University) for use of their glovebox and Prof. Dobereiner (Temple University) for helpful discussions.

Appendix A. Supplementary Material

Supplementary material associated with this manuscript can be found in the online version at [insert link]. This file contains more detail on experimental procedures as well as NMR spectra used for key analyses discussed herein.

References and notes

1. Lyons, T.W., Sanford, M.S., *Chem. Rev*. 2010;110;1147.
2. Diccianni, J.B., Hu,C., Diao, T. *Angew.Chem.Int.Ed*. 2016;55; 7534.
3. Higgs, A.T., Zinn, P.J., Simmons, S.J., Sanford, M.S. *Organometallic*s. 2009;28:6142.
4. Higgs, A.T., Zinn, P.J., Sanford, M.S. *Organometallics.* 2010;29: 5446.
5. Camasso, N.M., Sanford, M.S. *Science.* 2015;347:1218.
6. Silva, F.C.S., Tierno, A.F., Wengryniuk, S.E. *Molecules.* 2017; 22:780.
7. Martinez, G.E.; Ocampo, C.; Park, A.R. *J Am Chem Soc.* 2016; 138:4290.
8. Lee.E., Hooker, J.M., Ritter,T. *J Am Chem Soc.* 2012;134:17456.
9. Ananikov, V.P. *ACS Catal.* 2015;5:1964.
10. Camasso, N.M.; Canty, A.J.; Ariafard, A.; Sanford, M.S. Organometallics. 2017;36;4382.
11. Iyanaga, M., Aihara,Y., Chatani, N. *J.Org.Chem*. 2014;79;11933.
12. Aihara, Y., Chatani, N. *J.Am.Chem.Soc.* 2013;135;5308.
13. Aihara, Y., Chatani, N. J.Am.Chem.Soc. 2014;136;898.
14. Koo, K.; Hillhouse, G.L. *Organometallics.* 1995;14:4421.
15. Koo, K.; Hillhouse, G.L. *Organometallics.* 1996;15:2669.
16. Koo, K.; Hillhouse, G.L. *Organometallics*. 1995;14:4421.
17. Meucci, E.A., Camasso, N.M., Sanford, M.S. *Organometallics.* 2017;36:247.
18. Bour, J.R., Camasso, N.M., Sanford, M.S. *J Am Chem Soc.* 2015; 137:8034.
19. Whitfield, S.L., Sanford, M.S. *J Am Chem Soc.* 2007;129:15142.
20. Muñiz, K., Streuff, J., Hövelmann, C.H., Nunez, A. *Angew Chem Int Ed.* 2007;46:7125.
21. Vechorkin, O., Csok, Z., Scopelliti, R., Hu, X. *Chem Eur J.* 2009; 15:3889.
22. Vechorkin, O., Hu, X. *Angew Chem Int Ed.* 2009;48:2937.
23. Vechorkin, O., Proust, V., Hu, X. *J Am Chem Soc.* 2009;131: 9756.
24. Vechorkin, O., Barmaz, D., Proust, V., Hu. X. *J Am Chem Soc.* 2009;131:12078.
25. Ren, P., Verchokin, O., Allmen, K., Scopelliti, R., Hu, X. *J Am Chem Soc.* 2011;133:7084.
26. Hu, X., *Chem Sci.* 2011;2:1867.
27. Vechorkin, O., Godinat, A., Scopelliti, R.., Hu, X. *Angew Chem Int Ed.* 2011;50:11777.
28. Garcia, P.M.P., Di Franco, T., Orsino, A., Ren, P., Hu,X. *Org Lett.* 2012;14:4286.
29. Breitenfeld, J., Ruiz, J., Wodrich, M.D., Hu, X. *J Am Chem Soc.* 2013;135:12004.
30. Breitenfeld, J., Wodrich, M.D., Hu, X. *Organometallics.* 2014;33: 5708.
31. Di Franco, T., Stojanovic, M., Keller, S., Scopelliti, R.., Hu, X. *Helv.Chim. Acta.* 2016;99:830.
32. Csok, Z., Vechorkin, O., Harkins, S. B., Scopelliti, R., Hu, X. *J Am Chem Soc.* 2008;130:8156.
33. Corbo, R., Georgiou, D. C., Wilson, D. J. D., Dutton, J. L. *Inorg Chem.* 2014;53:1690.
34. Corbo, R., Pell, T. P., Stringer, B. D., Hogan, C. F., Wilson, D. J. D., Barnard, P. J., Dutton, J. L. *J Am Chem Soc*. 2014;*136*:12415.
35. Use of (tolyl)I(OAc)$_2$ and (tolyl)ICl$_2$ ensured that incorporated aryl ring arose from scaffold and not oxidant. No incorporation of tolyl ring was observed.
36. GCMS and ^{1}H-NMR analyses were performed against commercial standards of appropriate C–X bond products.
37. Henry, M. C., Mostafa, M. A. B., Sutherland, A. *Synthesis.* 2017; *49*:4586.
38. Bai, G., Stephan, D. W. *Angew Chem Int Ed Engl*. 2007;46:1856.
39. For an example of Ni-catalyzed biaryl formation with diaryliodonium salts: Tamura, Y., Chun, M.-W., Inoue, K., Minamikawa, J. *Synthesis*. 1978:822.
40. Hwang, S.J., Powers, D.C., Maher, A.G., Anderson, B.L., Hadt, R.G., Zheng, S-L., Chen, Y-S., Nocera, D.G. *J Am Chem Soc.* 2015;137:6472.
41. After flash chromatography, the isolated yields confirmed the crude ^{1}H-NMR ratios with *(NNN)*-NiCl being isolated as free *(NNN)*-ligand **(SI-1)**.
42. Attempts to confirm ratios with isolated yields of **23** were unsuccessful due to conversion of (*NNN*)-NiPh (**18**) to **23** upon exposure to O$_2$ on chromatography.
43. We cannot rule out ligand dissociation to generate a pentacoordinate complex prior to C–N reductive elimination from complex **21**. Any attempts to probe this hypothesis by altering X and studying its effect on the rate of reductive elimination were not successful due to the near instantaneous rate of C–N bond formation.
44. Rettenmeier, C. A., Wenz, J., Wadepohl, H., Gade, L. H. *Inorg Chem.* 2016;*55*:8214.
45. Tuhin, P., Soumitra, A., Atanu, M.; Debabrata, M. *Chem Commun*. 2013:8362.
46. Weiss,R., Seubert, J. *Angew Chem Int Ed.* 1994;33:891.
47. Bielawki, M., Olofsson, B. *Chem.Commun*. 2007;2521.
48. Ren, P., Vechorkin, O., Csok, Z., Salihu, I., Scopelliti, R., Hu, X. *Dalton Trans.* 2011;40:8906.